

Influence of the Nb Growth Surface on the Allotropic Ti Phase  
Transformation in Nb/Ti/Nb Nanolaminates

Gregory B. Thompson – The University of Alabama

Li Wan – The University of Alabama

Xiao-xiang Yu – The University of Alabama

Deposited 11/12/2018

Citation of published version:

Thompson, G., Wan, L., Yu, X. (2016): Influence of the Nb Growth Surface on the Allotropic Ti Phase Transformation in Nb/Ti/Nb Nanolaminates. *Applied Physics Letters*, 109(11). DOI: <https://doi.org/10.1063/1.4962828>

## Influence of the Nb growth surface on the allotropic Ti phase transformation in Nb/Ti/Nb nanolaminates

Li Wan, Xiao-xiang Yu, and Gregory Thompson<sup>a)</sup>

Department of Metallurgical and Materials Engineering, The University of Alabama, Tuscaloosa, Alabama 35487-0202, USA

(Received 12 June 2016; accepted 2 September 2016; published online 14 September 2016)

As the thickness of a thin film is decreased, the interfacial structure becomes paramount and crystals can undergo phase transformations. Molecular dynamic simulations have been performed to capture how such transformation could occur under the growth surface of a film. An hcp to bcc transition in Ti for Ti/Nb multilayers was used as the case studies. The simulations had good agreement with experiments. The simulations further predicted a mixed phase state for Ti for particular equal layer thicknesses. *Published by AIP Publishing.*  
[\[http://dx.doi.org/10.1063/1.4962828\]](http://dx.doi.org/10.1063/1.4962828)

Materials structures with large surface area-to-volume ratio such as thin films can exhibit size dependent physical and chemical properties<sup>1,2</sup> that are different from their bulk form. These properties enable devices with exceptional functionality to be developed, including capacitors,<sup>3,4</sup> optical switches,<sup>5,6</sup> and magnetic sensors.<sup>7,8</sup> Many of these changes are related to the material adopting a different crystallographic structure.<sup>9–15</sup> In multilayered thin films, the stability of different phases have been investigated through thermodynamic approaches<sup>16–19</sup> by determining the lowest energy configuration. However, the kinetic path that allows that phase to be achieved is not readily apparent. Since the growth of a thin film is a very dynamic process,<sup>20</sup> it is critical to understand how it impacts the pseudomorphic phase evolution. In this letter, we provide Molecular Dynamic (MD) simulations of thin film growth to understand possible sub-growth surface phase transformations.

According to the classic thermodynamic model of Dregia *et al.*<sup>16</sup> for phase stability in a multilayered thin film, the stabilization is governed by a competition between volumetric and interfacial energy penalties. In the multilayer stacking of two species, the layer thickness of each can be represented as the volume fraction of that layer multiplied to the combined or bilayer spacing of both layers. Using this bilayer construction, the relative thermodynamics can then be easily expressed in terms of the volumetric and interfacial energies within the bilayer. For example, consider the growth of Ti/Nb, our case study for this letter. Here, we will fix the volume fraction of each layer to be 0.5 or equal layer thicknesses where it has been previously reported<sup>15,18,21</sup> that hcp Ti adopts a bcc Ti phase. This could be expected as Ti undergoes  $\alpha$ -hcp to  $\beta$ -bcc polymorphic transformation with temperature in the bulk form. Here, as a multilayer, the total free Gibbs energy change per area in the bilayer,  $\Delta g_T$ , has only one degree of freedom, which is the bilayer thickness  $\lambda$ . This is expressed fully as

$$\Delta g_T = (\Delta G_{Ti} \times 0.5)\lambda + 2\Delta\gamma, \quad (1)$$

where  $\Delta G_{Ti}$  is the volumetric free energy change from  $\alpha$  to  $\beta$  and  $\Delta\gamma$  is the interfacial energy change with that change in phase at the interface. The two represents the interface below and above the Ti layer that is in contact with Nb. The deviation from the equilibrium  $\alpha$ -hcp phase to  $\beta$ -bcc will result in an energy penalty or positive change in volumetric energy. This is offset by the reduced interfacial energy change, which must be negative, to stabilize the pseudomorphic bcc Ti at ambient temperature and atmosphere.

One of the outstanding questions concerning this model and predictions for transformations<sup>17,22</sup> would be the possibility that the phase transformation occurs after its growth and below the new growth surface. According to Equation (1), strictly speaking, the stabilization of the pseudomorphic phase requires two interfaces. During its growth, in this case Ti, it would only be in contact with one bcc Nb interface. Only upon ceasing the deposition and the growth of a new Nb layer on the now deposited Ti surface would the second interface be manifested to Ti. This would imply the possibility that Ti could grow and adopt an hcp phase only to undergo a bcc transformation at a later stage of growth of the film. As such, an experimental *in situ* study would be difficult; we have explored the use of a MD simulation to study when the transformation in Ti would occur for various bilayer thicknesses. Simulations of thin film growth processes present an attractive and unique means to gain a deeper insight into this phase stability. Using the computational information, we performed post-mortem diffraction analysis of the selected experimental films to verify and validate the MD predictions. Through correlated computational and experimental approaches, the behavior between the hcp and bcc transformation in Ti/Nb can then be more fully realized.

The MD simulations were performed using LAMMPS: Large-scale Atomic/Molecular Massively Parallel Simulator<sup>23</sup> code with the embedded atom method (EAM) potential model<sup>24</sup> used for the Ti-Nb system from Ref. 25. Periodic boundary conditions were used for the two in-plane coordinate directions or growth surface to minimize the effect of small length scales in these two particular directions. To simulate the growth, a free boundary condition was used for the third coordinate direction. Vapor deposition is then simulated by continuously injecting adatoms towards

<sup>a)</sup> Author to whom correspondence should be addressed. Electronic mail: gthompson@eng.ua.edu

the free surface of the crystal at a frequency determined by the deposition rate. Because MD simulations solves for atom vibrations, the time step must be less than the shortest lattice vibration period (typically, a Debye frequency of around  $10^{-15}$  s). Consequently, an accelerated rate of deposition is used in order to deposit enough atoms in the available computational time to reveal structural features.<sup>26</sup> To prevent the simulated crystal from shifting because of the momentum transfer during adatom impact, several monolayers of atoms at the other free surface are fixed. Further details of the simulation can be found in Ref. 21.

In a previous work reported in Ref. 21, a MD simulation was used to match the phase transformation observed experimentally in a Ti/Nb multilayer. In that work, a simulated 1 nm Ti layer in contact with Nb substrate retained a bcc structure. When the Ti layer was 2 nm, a large portion of the Ti layer converted to a bulk, hcp phase, in contradiction to what was observed experimentally in terms of its growth stress response. To reconcile this difference, the MD simulation had not accounted for intermixing within the layers. Using prior reports from experimentally deposited Ti/Nb films characterized by atom probe tomography, it was revealed that Nb intermixes into the Ti layer to approximately 20 at.%, with the details of this intermixing and characterization found in Refs. 18 and 21. Using this information, the simulation was refined to include a Ti layer that has 20 at. % Nb. Here, the 2 nm Ti-20 at. % Nb layer was able to stabilize the bcc phase at 2 nm without a top surface growth surface of Nb. Assuming the intermixed Ti-20 at. % Nb layer was a regular solution, the entropy of the mixing was written as

$$\begin{aligned}\Delta S_{mix} &= -nR(a \ln a + b \ln b) \\ &= -nR(a \ln a + (1-a) \ln(1-a)).\end{aligned}\quad (2)$$

Since  $a$  is less than 1 in a binary mixing system and  $\Delta S_{mix}$  is positive. For this intermixed layer, the thermodynamic stability is dependent on the formation enthalpy. Raabe *et al.*<sup>27</sup> have employed *ab initio* simulations to Ti-Nb alloys and reported that the formation energy is always negative when Nb concentration are higher than 20 at. %. Thus, for the

multilayer, this mixing helped to reduce the volumetric energy change penalty for the  $\beta$  phase stabilization.

Though these simulations were useful in providing a confirmation of the phases observed, it did not develop insights into how phase stability involves nor the details if the top growth surface of Nb has any influence on the Ti's transformation under its surface, even though the thermodynamics from Equation (1) suggests an equivalent impact by having two interfacial energy reduction terms in the energy balance. This letter provides an in depth computationally driven investigation in how that top surface layer influences the phase stability of the sub-surface phase.

Fig. 1 is a series of simulated images that captures how the Ti layer evolves as subsequent layers of Nb are grown on its surface. Here, the Ti layer is grown on a polycrystalline Nb substrate and is intermixed to the experimentally known Ti-20 at.%Nb value. For the balance of the letter, this layer will be referred to as the mixed Ti layer as it is representative to the prior experimental findings. The top subfigures are colored by the element while the bottom subfigures are colored by the crystallographic structures using the common neighbor analysis (CNA) method.

Fig. 1(a) reveals that as the mixed Ti layer reaches  $\sim 3$  nm, the bcc phase destabilizes and the majority film's crystallography adopts the hcp structure, even in the mixed state. By growing  $\sim 0.5$  nm of Nb onto this surface, portions of the intermixed Ti layer qualitatively appear to show more bcc stabilization (Fig. 1(b)). This provides hints of how a new growth surface alters the phase stability of the previously deposited layer. Further incremental increasing of the Nb thickness up to  $\sim 3$  nm reveals this bcc stabilization in the mixed Ti layer (Figs. 1(c)–1(g)). Comparing the equivalent bilayer fraction between the  $\sim 3$  nm mixed Ti/ $\sim 3$  nm Nb, Fig. 1(g), to the  $\sim 2$  nm mixed Ti/ $\sim 2$  nm Nb, Fig. 1(h), the larger equivalent thicknesses qualitatively appear not to yield a complete bcc stabilized phase as compared to its thinner equivalent thickness counterpart.

To quantify this change of bcc and hcp coordination of the mixed Ti layer, Fig. 2(a) quantitatively reveals how the bcc and hcp coordination of the Ti changes with increasing

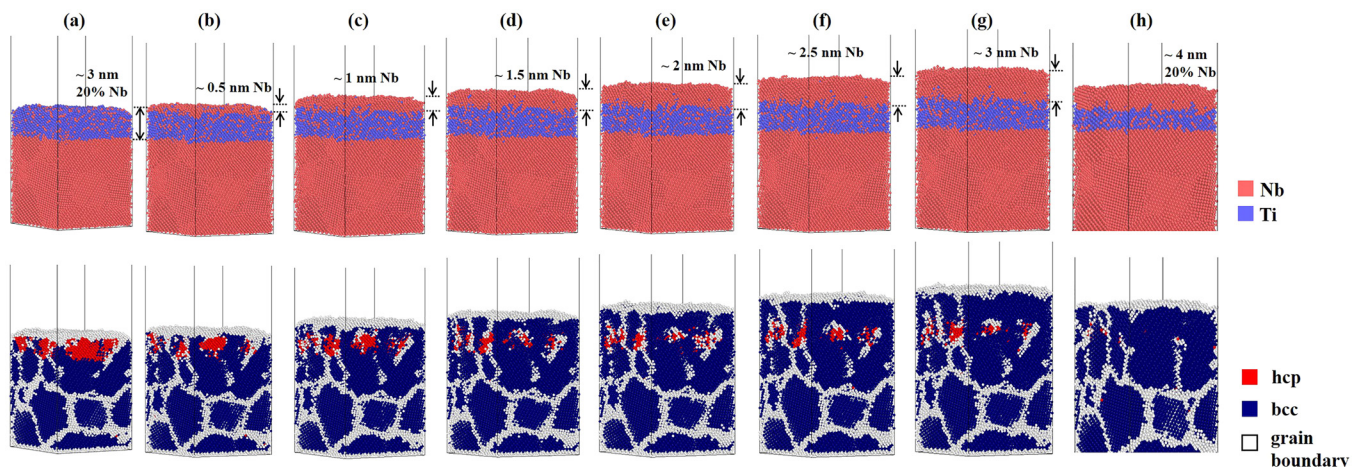


FIG. 1. MD simulation of 3 nm Ti/3 nm Nb multilayer deposition. The Nb layer thickness is increased at a 0.5 nm interval up to 3 nm. (a) Initial 3 nm mixed Ti layer on Nb. (b) 0.5 nm Nb on 3 nm mixed Ti layer. (c) 1 nm Nb on 3 nm mixed Ti layer. (d) 1.5 nm Nb on 3 nm mixed Ti layer. (e) 2 nm Nb on 3 nm mixed Ti layer. (f) 2.5 nm Nb on 3 nm mixed Ti layer. (g) 3 nm Nb on 3 nm mixed Ti layer. (h) 2 nm Nb/2 nm Ti (with 20 at. % Nb mixing) on Nb. (a) and (h) were reproduced with permission from Wan *et al.*, Acta Mater. **80**, 490 (2014). Copyright 2014 Acta Materialia Inc.

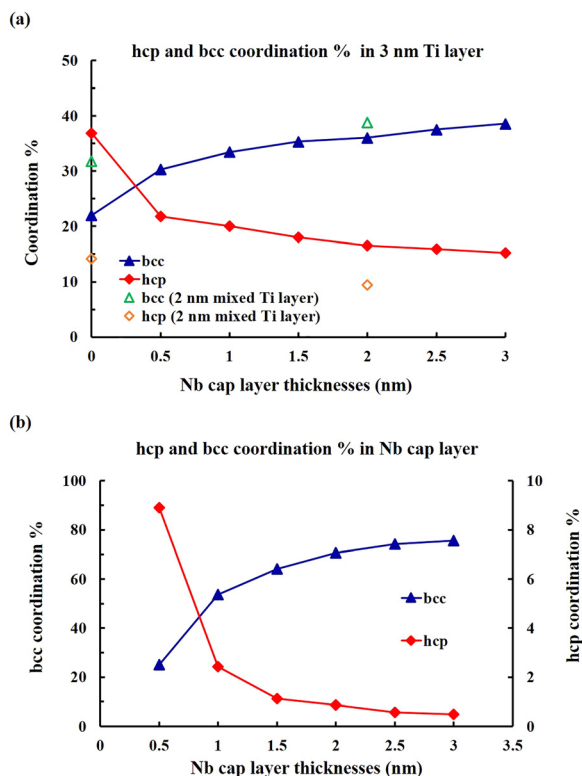


FIG. 2. (a) hcp and bcc coordination percentage (%) in the 3 nm Ti layer. The bcc and hcp coordination percentage in 2 nm mixed Ti layer are plotted for comparison. (b) hcp and bcc coordination percentage in the Nb top layer versus the Nb cap layer thickness in the 3 nm Ti/3 nm Nb multilayer.

Nb layer thickness on its surface. For comparison, the values for the  $\sim 2$  nm mixed Ti layer at the initial condition (i.e., no Nb top surface), and at its equivalent layer thickness of a  $\sim 2$  nm Nb top surface, Fig. 1(h), are also included on this plot. As the Nb layer grew on the  $\sim 3$  nm mixed Ti layer, the mixed Ti stabilized a larger fraction of its atoms as bcc. However, this bcc stabilization is not complete throughout the  $\sim 3$  nm of Nb top surface growth. The largest extent of bcc stabilization occurred within the first  $\sim 1.5$  nm of Nb growth on the  $\sim 3$  nm mixed Ti surface. Arguably, the majority of prior literature on multilayer phase transformations has suggested that these layers are either all or not transformed. This simulation provides insight that the transformations, within a single layer, may be a mixed phase. Since the very thin Ti layers can undergo a transformation, the coordination of the Nb layer on the  $\sim 3$  nm mixed Ti surface is also plotted in Fig. 2(b). Here, the majority of the Nb atoms adopt an hcp coordination at layer thicknesses less than 1 nm. Thompson *et al.* has reported for very thin Nb in Zr/Nb multilayers, hcp Nb stabilization occurs.<sup>17</sup>

To confirm that the hcp phase (or a portion thereof) is indeed stabilized for a 3 nm Ti/3 nm Nb multilayer, such a film was sputter deposited under the conditions reported previously.<sup>21</sup> Since this film was grown in a manner similar to the prior report, the intermixing between the layers occurred. We note that the growth of Ti/Nb on a completely different sputtering system revealed similar and reproducible levels of intermixing;<sup>18</sup> this intermixing appears to be a common feature of this multilayer regardless of the chamber from which it is sputtered. The Transmission Electron Microscopy

(TEM) plan view and cross-sectional images are shown in Figs. 3(a) and 3(b). The inset diffraction pattern in the plan view orientation for the experimental film does indeed show the hcp Ti phase reflections. For comparison, the 2 nm Ti/2 nm Nb plan view and cross-sectional image is given in Figs. 3(c) and 3(d) and its inset diffraction pattern revealed only bcc stabilization (note the clear absence of the  $\{10\bar{1}0\}$  reflection seen in the prior pattern). These experimental diffraction reports confirm the prior simulation findings in Fig. 1 and those reported in Ref. 21.

One of the challenges in determining if bcc Ti is also stabilized with hcp Ti in a single layer for the 3 nm/3 nm multilayer is that  $\beta$ -Ti and bcc Nb have near equivalent lattice parameters resulting in overlapping reflections. Attempts at dark field imaging bcc grains in the Ti layer were attempted and found not to be possible. The  $\{0002\}$  hcp Ti d-spacing of 0.2341 nm (ICDD PDF 00-044-1294) is very near the  $\{110\}$  bcc Nb 0.2338 nm (ICDD PDF 00-035-0789) value. By selecting the  $\{110\}$  reflection for imaging, the close-packed reflection could also be captured. Thus, any grains that are imaged in the Ti layer could be either  $\beta$ -Ti or hcp Ti. Unlike the plan-view condition, where the electron beam is parallel to this close packed hcp direction and the diffraction condition for these reflections are not satisfied; in the cross-section, the electron beam is now perpendicular to this direction and satisfies the diffraction condition. However, similar d-spacing values for other hcp and bcc reflections had similar near close proximity issues where the smallest aperture in the TEM could not separate only bcc symmetric reflections. Consequently, any dark film imaging of grains in the Ti could not be conclusive as bcc in the layer, as it could be either bcc or hcp. High resolution TEM was also found to be inconclusive because bcc and hcp share a similar ABAB stacking in the close packed direction, which these films grew,<sup>21</sup> and have near similar d-spacings as noted above. Regardless of these experimental

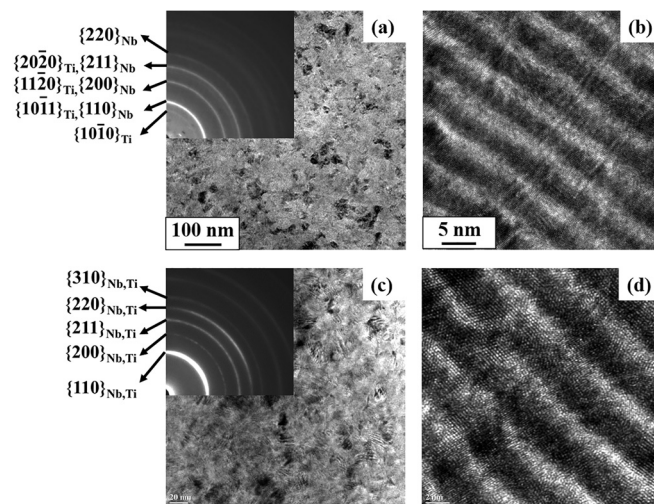


FIG. 3. (a) Plan-view TEM image of the 3 nm Ti/3 nm Nb multilayer. The inset is the electron diffraction pattern taken on this multilayer. Note that the distinctive hcp Ti ring has determined this multilayer to be hcp/bcc Ti/Nb. (b) Cross-section TEM image of the 3 nm/3 nm multilayer. (c) Plan-view TEM image of the 2 nm Ti/2 nm Nb multilayer. The inset is the electron diffraction pattern taken on this multilayer. The extinction of the hcp confirms the bcc/hcp phase in this multilayer. (d) Cross-section TEM image of the 2 nm/2 nm multilayer. The interface remains sharp.

challenges, the agreement of the simulation for the existence of the hcp phase provides confidence in its predictive capability and support for the possibility of mixed phase layers within these types of multilayers. It also demonstrates the importance of simulations in being complimentary to experimental findings in resolving phase stability. Even though these simulations addressed a bilayer structure, where the multilayers themselves involve a series of bilayer stacks, the thermodynamic framework of Equation (1) is sufficient in capturing the correct physics of the unit structure, as long as each unit structure is consistent in its layer thickness with each other as it grows.

In summary, a MD deposition code was used to investigate the phase stability in a Ti/Nb multilayer. The simulations were able to provide insight into the possibility of sub-growth surface transformations within the Ti layer as a result of a second bcc Nb interface. The results revealed that Ti, in a 2 nm/2 nm configuration, was nearly completely stabilized as bcc Ti, which agreed with the experiments. However, a 3 nm/3 nm configuration resulted in mixed bcc and hcp phase predictions for the Ti layer. This hcp phase was confirmed experimentally; however, conclusive determination of the bcc Ti within the Ti layer was elusive because of similar diffraction reflections between  $\beta$ -Ti and  $\alpha$ -Ti. This work demonstrates how simulations can provide further insight into the stability behavior of nanoscale thin film materials, particularly when experimental methods are unable to capture the event.

This work has been supported by the National Science Foundation (Grant No. NSF-DMR-1207220). The authors thank the Central Analytical Facility in the University of Alabama for support.

- <sup>1</sup>F. Wu and J. Narayan, *Cryst. Growth Des.* **13**, 5018 (2013).
- <sup>2</sup>C. B. Parker, J.-P. Maria, and A. I. Kingon, *Appl. Phys. Lett.* **81**, 340 (2002).
- <sup>3</sup>K. Natori, D. Otani, and N. Sano, *Appl. Phys. Lett.* **73**, 632 (1998).
- <sup>4</sup>D. V. Bavykin, J. M. Friedrich, and F. C. Walsh, *Adv. Mater.* **18**, 2807 (2006).
- <sup>5</sup>S. Zhang, M. A. Kats, Y. Cui, Y. Zhou, Y. Yao, S. Ramanathan, and F. Capasso, *Appl. Phys. Lett.* **105**, 211104 (2014).
- <sup>6</sup>T. Fukaya, J. Tominaga, T. Nakano, and N. Atoda, *Appl. Phys. Lett.* **75**, 3114 (1999).
- <sup>7</sup>J. Shen and J. Kirschner, *Surf. Sci.* **500**, 300 (2002).
- <sup>8</sup>J. Shen, Z. Gai, and J. Kirschner, *Surf. Sci. Rep.* **52**, 163 (2004).
- <sup>9</sup>L. Wilson and A. Bienenstock, *MRS Proc.* **103**, 69 (1987).
- <sup>10</sup>P. Boher, F. Giron, Ph. Houdy, P. Beauvillain, C. Chappert, and P. Veillet, *J. Appl. Phys.* **70**, 5507 (1991).
- <sup>11</sup>W. Vavra, D. Barlett, S. Elagoz, C. Uher, and R. Clarke, *Phys. Rev. B* **47**, 5500 (1993).
- <sup>12</sup>Y. Li, J. Li, and B. Liu, *Acta Mater.* **93**, 105 (2015).
- <sup>13</sup>Y. Li, J. Li, and B. Liu, *Phys. Chem. Chem. Phys.* **17**, 4184 (2015).
- <sup>14</sup>W. Zhang, W. S. Zhao, D. X. Li, and M. L. Sui, *Appl. Phys. Lett.* **84**, 4872 (2004).
- <sup>15</sup>L. Wan, X.-X. Yu, X. Zhou, and G. Thompson, *J. Appl. Phys.* **119**, 245302 (2016).
- <sup>16</sup>S. A. Dregia, R. Banerjee, and H. L. Fraser, *Scr. Mater.* **39**, 217 (1998).
- <sup>17</sup>G. B. Thompson, R. Banerjee, S. A. Dregia, and H. L. Fraser, *Acta Mater.* **51**, 5285 (2003).
- <sup>18</sup>G. B. Thompson, R. Banerjee, S. Dregia, M. K. Miller, and H. L. Fraser, *J. Mater. Res.* **19**, 707 (2004).
- <sup>19</sup>J. C. Li, W. Liu, and Q. Jiang, *Acta Mater.* **53**, 1067 (2005).
- <sup>20</sup>R. Q. Hwang and M. C. Bartelt, *Chem. Rev.* **97**, 1063 (1997).
- <sup>21</sup>L. Wan, X.-X. Yu, and G. B. Thompson, *Acta Mater.* **80**, 490 (2014).
- <sup>22</sup>R. Banerjee, R. Ahuja, and H. L. Fraser, *Phys. Rev. Lett.* **76**, 3778 (1996).
- <sup>23</sup>S. Plimpton, *J. Comput. Phys.* **117**, 1 (1995).
- <sup>24</sup>M. S. Daw and M. I. Baskes, *Phys. Rev. B* **29**, 6443 (1984).
- <sup>25</sup>L. Ward, A. Agrawal, K. M. Flores, and W. Windl, preprint [arXiv:1209.0619](https://arxiv.org/abs/1209.0619) (2012).
- <sup>26</sup>X. W. Zhou and H. N. G. Wadley, *Surf. Sci.* **431**, 42 (1999).
- <sup>27</sup>D. Raabe, B. Sander, M. Friák, D. Ma, and J. Neugebauer, *Acta Mater.* **55**, 4475 (2007).